Pressure-Dependent FTIR-Spectroscopy on the Counterbalance between External and Internal Constraints in Spider Silk of Nephila pilipes

ARTICLE *in* MACROMOLECULES · JUNE 2013

Impact Factor: 5.8 · DOI: 10.1021/ma400498v

8 AUTHORS, INCLUDING:

Wilhelm Kossack
University of Leipzig
16 PUBLICATIONS **108** CITATIONS
SEE PROFILE

Christof Gutsche
University of Leipzig
26 PUBLICATIONS **375** CITATIONS
SEE PROFILE

Roxana Figuli
Karlsruhe Institute of Technology
13 PUBLICATIONS **135** CITATIONS
SEE PROFILE

Periklis Papadopoulos
University of Ioannina
54 PUBLICATIONS **984** CITATIONS
SEE PROFILE

Macromolecules

Article

pubs.acs.org/Macromolecules

Pressure-Dependent FTIR-Spectroscopy on the Counterbalance between External and Internal Constraints in Spider Silk of *Nephila pilipes*

Arthur Markus Anton,[†,*] Wilhelm Kossack,[†] Christof Gutsche,[†] Roxana Figuli (Ene),[‡] Periklis Papadopoulos,[§] Jihaan Ebad-Allah,[⊥] Christine Kuntscher,[§] and Friedrich Kremer[†]

[†]Institut für Experimentelle Physik I, Universität Leipzig, Linnéstraße 5, D-04103 Leipzig, Germany, e-mail: anton@physik.uni-leipzig.de

[‡]Institut für Technische Chemie und Polymerchemie, Karlsruher Institut für Technologie, Engesserstraße 18, D-76128 Karlsruhe, Germany

[§]Max Planck Institut für Polymerforschung, Ackermannweg 10, D-55128 Mainz, Germany

[⊥]Institut für Physik, Universität Augsburg, Universitätsstraße 1, D-86159 Augsburg, Germany

ABSTRACT: Nanocrystals composed mainly of β-sheet polyalanine are responsible for the high toughness of major ampullate (dragline) spider silk. Fourier-transform infrared (FTIR) spectroscopy is employed to study their response to (i) uniaxial stress and (ii) hydrostatic pressure. In the former a red shift and in the latter a blue shift of the vibration of polyalanine β-sheets at 965 cm^{-1} occurred. In both cases, a linear dependence is observed, which bends off for hydrostatic pressure greater than 1.4 GPa and is fully reversible up to 7 GPa. The seamless connection of negative and positive pressure regimes corroborate quantitatively our structural model of spider silk as composed of *prestressed* alanine-rich nanocrystals embedded in a glycine-rich amorphous matrix. It is also confirmed that nanocrystals withstand high pressures without undergoing structural transition or deteriorating their mechanical properties.

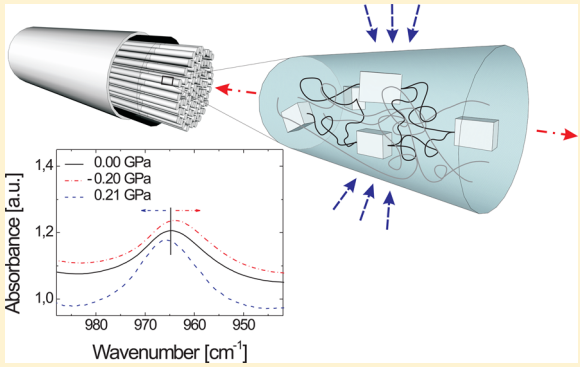

INTRODUCTION

Spider dragline (major ampullate) silk has the highest toughness ever observed for any material.[1,2] It consists mainly of two proteins, MaSp1 and MaSp2 (major ampullate spidroin 1 and 2), both being copolymers with glycine- and alanine-rich motifs.[3,4] They are spun in the gland from a highly concentrated solution undergoing ion exchange (e.g., chloride and sodium), pH change, and water segregation, while being exposed to shear forces.[5,6] Several attempts were made to develop silk-mimicking materials by synthetic or recombinant proteins.[7−9] Proposed applications, including bullet-proof vests, require that these materials withstand pressures of several GPa.[10]

The structure of spider silk has been studied by a variety of experimental techniques, including X-ray scattering,[11−14] infrared (IR),[15−18] and Raman spectroscopy,[19,20] as well as nuclear magnetic resonance (NMR),[21−23] to unravel the molecular origin of the extraordinary mechanical properties. There is general agreement that spider silk is reinforced by hard crystalline segments—approximately 40% of the fiber's volume is made of alanine-rich blocks forming highly oriented β-sheet crystals with size of about a few nanometers.[16,21,24−27] They are embedded and interconnected in predominantly serial arrangement by amorphous glycine-rich chains,[12,28,29] of which a fraction is *prestressed*.[17] The resulting net force is counterbalanced by the surrounding amorphous glassy matrix and the external skin.[16−18,30] As a result, reeling speed affects the modulus of spider silk.[31] Recent simulations on nanocrystals with similar composition and size showed that there is an optimal size of the nanocrystals with respect to the toughness of silk.[32,33] Despite the fact that stress applied to silk during stretching experiments reaches about 1 GPa, the effects of higher pressures and the possibility of failure of the nanocrystals have not been investigated experimentally.

FTIR-spectroscopy in combination with external mechanical fields (unidirectional stress or hydrostatic pressure) is a suitable tool to gain insight into the structural organization of spider's (major) ampullate silk. The nonoverlapping N−C$_\alpha$ polyalanine stretching vibration at $\bar{\nu}$ = 965 cm^{-1} can be used as molecular sensor of relative force changes within the β-sheet nanocrystals.[16] Hence, one is able to study the microscopic response to external mechanical fields through the observation of shifts of this vibration.[16−18,30] Here both stretching and pressing experiments are performed on the same material. Thus, the

Received: March 8, 2013
Revised: April 11, 2013
Published: June 11, 2013

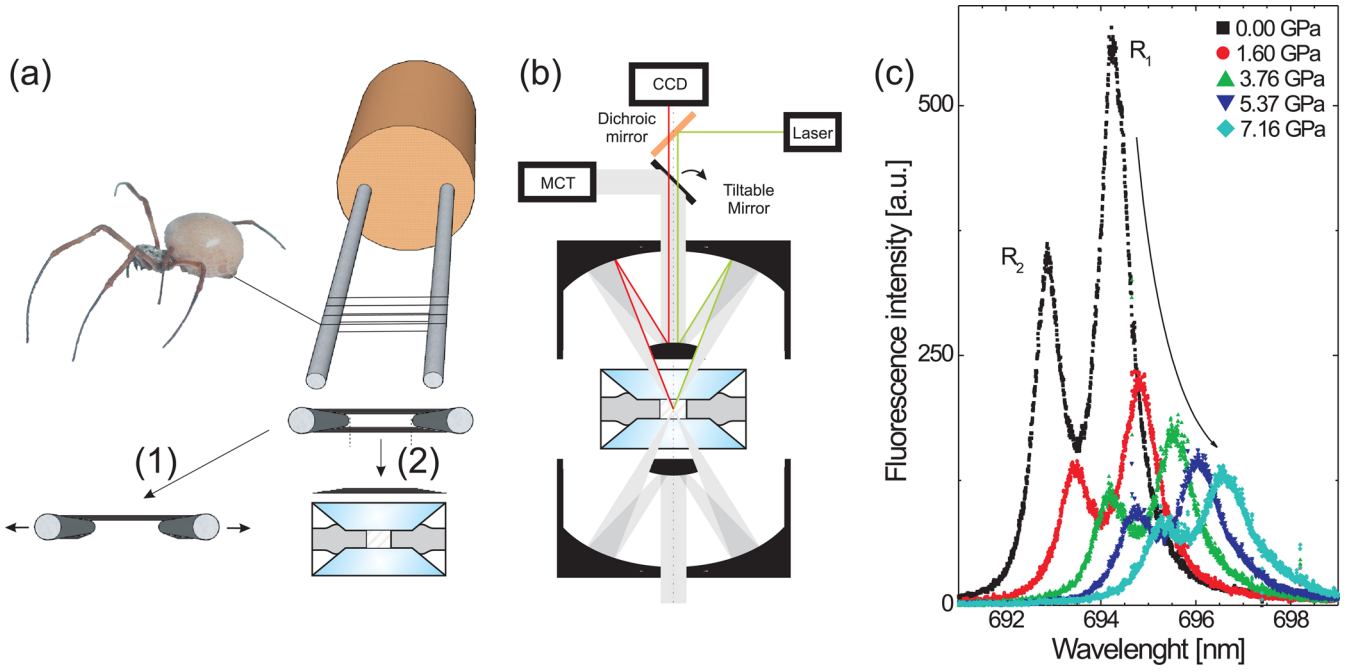

Figure 1. (a) Sample preparation and experimental setup. A spider's major ampullate fiber is forcibly silked and wound around two rods resulting in an aligned double-sided grid of fibers. After fixing the fibers to the rods, the lower side of the grid is cut off and taken for the pressure-dependent experiment (2). The upper one is used for the stress-dependent experiment (1). (b) Pressure-dependent FTIR spectroscopy setup using a diamond anvil cell. IR-light is focused on the sample by Cassegrain optics and measured with a mercury−cadmium−telluride (MCT) detector. In order to determine the hydrostatic pressure in the sample cell, the fluorescence of embedded ruby particles (15 to 60 μm diameter) is excited with a green laser at 532 nm and detected through the same light-path as used for the IR-measurements. (c) Ruby fluorescence versus (vs) wavelength. The lines R_1 and R_2 are shifted to lower energy with increasing hydrostatic pressure.

stability of the nanocrystals and the way they are connected with the amorphous phase can be better understood.

EXPERIMENTAL SECTION

The samples are made of major ampullate (dragline) silk from the spider *Nephila pilipes* gained by forced silking. A detailed description of this procedure can be found elsewhere.[16] The spiders were fed with crickets. Diet variation may affect the total content of alanine but only marginally the fraction of β-sheets.[34] *N. pilipes* MaSp1 and MaSp2 spidroins have alanine-rich groups that are about 7−8 residues long,[35] whereas *Nephila madagascariensis* in our previous studies[17,30] had about 9−10.[4]

A thread of silk is precisely wound around two rods by means of a motorized stage controller resulting in a double-sided dense grid of 400 aligned fibers each side (Figure 1a). Using a Dektak 3030 profilometer the diameter of the threads is determined to be 4.6 μm for one sample and (6.9 ± 0.3) μm for the other by taking the average of 4 to 6 measurements at different positions along the thread. For stress-dependent experiments the silk threads are glued to the rods, around which they are wound, and one side of the double-sided grid is cut off, see Figure 1a(1). Afterward, the fibers are wetted with paraffin oil (Fluka) in order to minimize scattering. Previous measurements revealed that this treatment does not alter the mechanical properties of the sample.[16] For pressure-dependent experiments, the threads removed (cut off) from the stretching experiment (Figure 1a(2)) are placed—without any alignment—in the hole of a gasket. Ruby powder (15 to 60 μm diameter, easyLab) is added for pressure determination[36] and the same paraffin oil as for stretching experiments is employed as pressure transmitting medium providing hydrostatic conditions at least up to 5 GPa.[37] Care is taken to avoid any exposure of the sample to stress or pressure prior to the measurement, except for that inevitable during forced silking.

FTIR measurements are performed in transmission mode on a Bio-Rad FTS 6000 FTIR-spectrometer equipped with a UMA-500 infrared microscope. The infrared light is focused on the sample by means of Cassegrain optics and measured by a mercury−cadmium−telluride (MCT) detector (Kolmar Technologies) with a spectral resolution of 1 cm^{-1}. For stress-dependent experiments the fibers are stretched using micrometer screws. The resulting force is measured by a force sensor (8411−10, Burster GmbH). A detailed description of this measurement technique can be found elsewhere.[16] Hydrostatic pressure is applied by means of a Diacell μScopeDAC-HT(G) diamond anvil cell (DAC) manufactured by easyLab. Synthetic type 2a diamonds with a culet size of 600 μm and a steel gasket with an initial thickness of 250 μm are employed. A hole of 300 μm diameter is drilled into the gasket after preindentation to roughly 60 μm.[38] Additional information about high-pressure transmission studies can be found in references.[39,40]

Hydrostatic pressure is determined *in situ* from the pressure-dependent shift of the ruby R_1 and R_2 fluorescence lines.[41] For that, ruby crystals are excited using green laser light at 532 nm (Nano 250−532−100, Qioptiq) which is guided through an additional port of the infrared microscope (Figure 1b). The fluorescence light is separated from the excitation radiation using a dichroic mirror (MPL567, Thorlabs). The ruby fluorescence spectrum (Figure 1c) is measured by means of a grating spectrometer (SpectraPro-750, Acton Research Corporation, 1800 lines/mm) equipped with a CCD line array camera (Larry 3000, LOT Oriel, 7 μm pixel width). Because of a fine grating and small pixels, hydrostatic pressure within the sample cell can in principle be determined with a resolution of at least 15 MPa.

The spectral position of the alanine-specific vibration in the β-sheet nanocrystals at $\overline{\nu}$ = 965 cm^{-1} [16,42,43] is determined by fitting the absorbance spectra with a Gaussian profile. A superposition of two additional Gaussian profiles modeling the adjacent flanks of the neighboring peaks is chosen as baseline. In stretching experiments, the true applied stress per fiber σ is calculated based on the measured force assuming constant fiber volume[30,44]

$$\sigma = \frac{4}{\pi n d_0^{\,2}} F(1 + \varepsilon)$$

dx.doi.org/10.1021/ma400498v | *Macromolecules* 2013, 46, 4919−4923

where F represents the measured force, n the number of fibers, ε the applied strain, and d_0 the diameter of one fiber at 0% strain. This stress is considered as a negative pressure to emphasize the analogy between stretching and pressure-dependent experiments. For the latter pressure is evaluated from the shift of the fluorescence line R_1 (Figure 1c), according to the ruby pressure scale (RPS).[36,41,45] Temperature-induced shifts (ΔT < 2 K) are corrected[46] and effects caused by asymmetric line shapes (appearing at p < 2 GPa) are taken into consideration resulting in a small modification (Δp < 10 MPa).[47]

RESULTS AND DISCUSSION

Representative FTIR spectra of pressurized spider silk are depicted in Figure 2a. Besides the prominent diamond

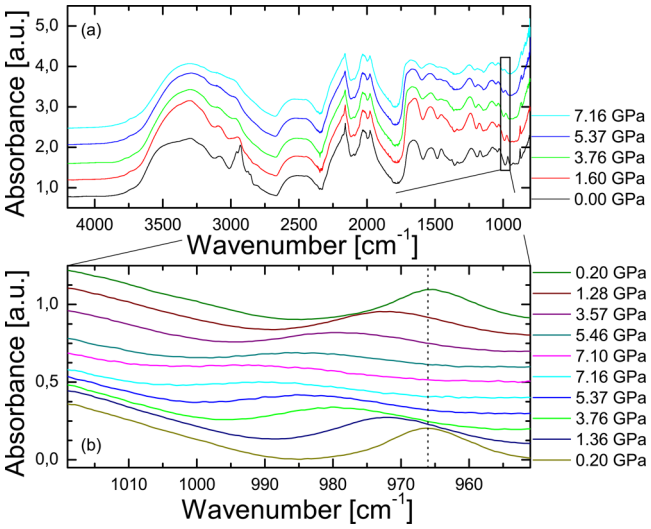

Figure 2. (a) IR-absorbance spectra of major ampullate silk at different hydrostatic pressures. The spectrum is dominated by the amide I, II, and N−H stretching bands. The box marks the region of interest around the β-sheet polyalanine vibration. (b) The shift of the polyalanine absorption peak to higher wavenumbers with increasing hydrostatic pressure is fully reversible and demonstrates the reproducibility of the measurement. For graphical reasons all spectra are shifted vertically. The corresponding spectra are in the same order as the pressure values in the legend at the side. For comparison, the vertical line shows the position of the band at 0.2 GPa.

absorption (1700 cm^{-1} < $\bar{\nu}$ < 2700 cm^{-1}), amide I, II, and N−H stretching bands are visible, but saturated due to the thickness of silk. However, at lower wavenumbers amino acid- and structure-specific bands can be found. This includes the main-chain vibration within the β-sheet polyalanine nanocrystals that appears at $\bar{\nu}$ = 965 cm^{-1} without external load (Figure 2b).[16] This vibration frequency was shown to shift linearly with applied stress in static and dynamic stretching experiments by about −3 cm^{-1} GPa^{-1}, independent of sample history. The shift is due to anharmonicity of the bonds and provides a molecular sensor of force located *within* the nanocrystals. However, stretching does not ensure that macroscopic stress is equal to crystal stress. Supercontraction experiments[48] showed that crystal stress decreases, when silk shrinks spontaneously in the presence of water, proving the existence of *prestress* in unstretched native silk fibers in the order of 300 MPa.

The application of hydrostatic pressure gives rise to band shifts in the opposite direction. Pressure up to 1.4 GPa causes a linear blue shift of the peak position of the polyalanine vibration of about (5.4 ± 0.2) cm^{-1}GPa^{-1} (linear fit in the region 0.1−1.4 GPa in Figure 3). The origin of the plateau (0−

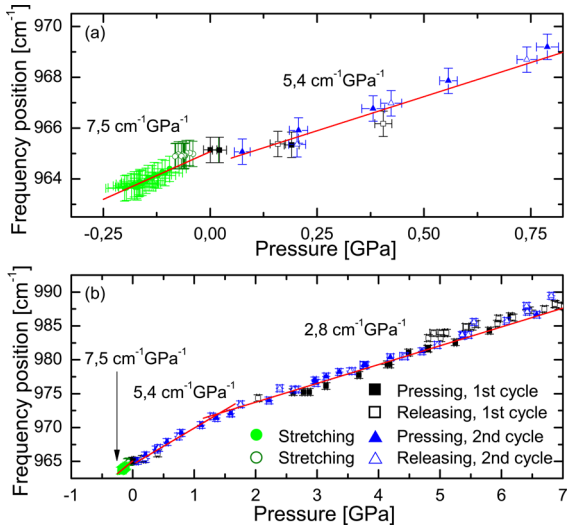

Figure 3. Spectral position of the polyalanine absorption band vs negative uniaxial pressure (caused by stretching the fibers) and vs positive hydrostatic pressure. Within experimental accuracy, the frequency shift is fully reversible. Panel a shows an enlargement of the low pressure region in part b.

73 MPa) is caused by the experimental impossibility to mount a stretched sample into the DAC (though, not included in the linear regression, the point at 73 MPa coincides with it). At 1.4 GPa (intersection of linear fits), a "kink" is observed where the slope of the frequency dependence changes to (2.8 ± 0.1) cm^{-1}GPa^{-1} (fit in region 2.0−5.0 GPa). The origin of the bending off in slope of the band shift is not yet understood. One possible argument could be the anisotropy of the nanocrystals' elastic moduli for which at 0.6 GPa a factor of 8 was found.[11] Hence, the external hydrostatic pressure might *not* be isotropic on a microscopic scale, an effect which is expected to be pressure dependent. A different explanation could be the inherent prestress of spider silk. While only pressure values up to 5.0 GPa ensure complete hydrostatic condition[37] and, hence, only points in this region are taken into consideration for a linear fit, the frequency shift up to 7 GPa follows this trend. The response is fully reversible (Figure 2b and Figure 3b) without any indications of hysteresis up to 10 GPa (data not shown), proving that the applied stress in silk is homogeneous at least in the hydrostatic limit. Thus, the measurements with hydrostatic pressure can be used to calibrate the frequency shift of the alanine vibration. Consequently, absolute values for the crystal stress are obtained also for the stretching experiments, where until now we could only *assume* that they were equal to the macroscopic stress. The linear dependence for pressures lower than 1.4 GPa coincides with the red shift observed in stretching measurements (7.5 ± 0.4 cm^{-1} GPa^{-1}) carried out on the identical sample material (Figure 3a). Differences of the slopes between stress- and pressure-dependent measurements suggest that tensile stress is not simply a negative pressure on the crystals. Under stress the nanocrystals are compressed laterally.

The nearly equal dependence of the vibration frequency on stress and pressure suggests that tensile stress and nanocrystals stress are equivalent and in full agreement with our structural model of spider silk[16−18] (Figure 4): Within a fibril, alanine-rich β-sheet nanocrystals are interlinked and embedded in glycine- and proline-rich amorphous chains, of which a fraction is *prestressed*. The resulting internal force is counterbalanced by

dx.doi.org/10.1021/ma400498v | *Macromolecules* 2013, 46, 4919−4923

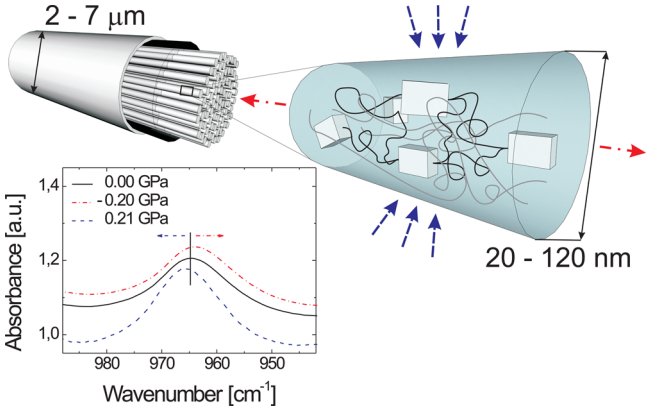

Figure 4. Schematic interpretation of the response of spider silk to external mechanical loads. Hydrostatic pressure (indicated by blue arrows) induces a blue shift of the polyalanine band, whereas uniaxial stress (red arrows) causes a red shift.

the surrounding matrix and the external skin. The alanine specific vibration reflects in its spectral position the relative changes in its potential, hence acting in our measurements as molecular sensor of force being located *within* the nanocrystals.

The equivalence of uniaxial tensile stress and isotropic hydrostatic pressure is not self-evident and may be explained by the low compressibility normal to the main peptide chain.[11] The deviation at hydrostatic pressures above 1.4 GPa is an indication that first order perturbation theory[16] is inadequate at elevated pressure. However, the absence of hysteresis or discontinuities proves that crystals are only elastically deformed retaining their structure up to 7 GPa without degradation of their mechanical properties.

CONCLUSION

The molecular force sensor in spider silk based on the shift of a polyalanine vibration in nanocrystals is employed for the first time under both tensile stress and hydrostatic pressure. We show that the effects of pressures up to 7 GPa on silk are reversible, allowing silk to retain its mechanical properties under extreme conditions. The observed coincidence in the pressure dependence under conditions of uniaxial stress or hydrostatic pressure proves the validity of our model for the structural organization of dragline spider silk.[16−18] Consequently, as next step, we plan to extend these studies to supercontracted[48,49] and hindered supercontracted[49] silk as well as to extend first order perturbation theory.[16]

AUTHOR INFORMATION

Corresponding Author

*E-mail: (M.A.) markus.anton@uni-leipzig.de.

Notes

The authors declare no competing financial interest.

ACKNOWLEDGMENTS

The authors would like to thank Jörg Reinmuth and Viktor Skokow for technical support during the construction of the measurement setup, Thomas Meier and Thomas Meissner for fruitful discussions regarding the DAC and gasket preparation, and Gabriele Ramm for help while determining the fibers' diameter. Financial support by the Deutsche Forschungsgemeinschaft DFG (Project B5 within the SFB/TRR 102) "Polymers under multiple constraints: restricted and controlled molecular order and mobility" and through the Leipzig School of Natural Sciences "Building with Molecules and Nano-Objects" (BuildMoNa) is highly acknowledged.

REFERENCES

(1) Kubik, S. *Angew. Chem., Int. Ed.* **2002**, *41*, 2721−2723.
(2) Fu, C.; Shao, Z.; Vollrath, F. *Chem. Commun.* **2009**, 6515−6529.
(3) Hayashi, C. Y.; Shipley, N. H.; Lewis, R. V. *Int. J. Biol. Macromol.* **1999**, *24*, 271−275.
(4) Gatesy, J.; Hayashi, C.; Motriuk, D.; Woods, J.; Lewis, R. *Science* **2001**, *291*, 2603−2605.
(5) Eisoldt, L.; Smith, A.; Scheibel, T. *Mater. Today* **2011**, *14*, 80−86.
(6) Vollrath, F.; Knight, D. P. *Nature* **2001**, *410*, 541−548.
(7) Hardy, J. G.; Römer, L. M.; Scheibel, T. R. *Polymer* **2008**, *49*, 4309−4327.
(8) Spiess, K.; Ene, R.; Keenan, C. D.; Senker, J.; Kremer, F.; Scheibel, T. *J. Mater. Chem.* **2011**, *21*, 13594−13604.
(9) Heim, M.; Keerl, D.; Scheibel, T. *Angew. Chem., Int. Ed.* **2009**, *48*, 3584−3596.
(10) Vlattas, C.; Galiotis, C. *Polymer* **1994**, *35*, 2335−2347.
(11) Ene, R.; Krywka, C.; Kang, S.-G.; Papadopoulos, P.; Burghammer, M.; Cola, E. D.; Müller, M.; Kremer, F. *Polymer* **2012**, *53*, 5507−5512.
(12) Glisovic, A.; Vehoff, T.; Davies, R. J.; Salditt, T. *Macromolecules* **2008**, *41*, 390−398.
(13) Riekel, C.; Vollrath, F. *Int. J. Biol. Macromol.* **2001**, *29*, 203−210.
(14) Miller, L. D.; Putthanarat, S.; Eby, R.; Adams, W. *Int. J. Biol. Macromol.* **1999**, *24*, 159−165.
(15) Dong, Z.; Lewis, R. V.; Middaugh, C. *Arch. Biochem. Biophys.* **1991**, *284*, 53−57.
(16) Papadopoulos, P.; Sölter, J.; Kremer, F. *Eur. Phys. J. E: Soft Matter Biol. Phys.* **2007**, *24*, 193−199.
(17) Papadopoulos, P.; Sölter, J.; Kremer, F. *Colloid Polym. Sci.* **2009**, *287*, 231−236.
(18) Ene, R.; Papadopoulos, P.; Kremer, F. *Soft Matter* **2009**, *5*, 4568−4574.
(19) Sirichaisit, J.; Brookes, V. L.; Young, R. J.; Vollrath, F. *Biomacromolecules* **2003**, *4*, 387−394.
(20) Rousseau, M.-E.; Lefèvre, T.; Beaulieu, L.; Asakura, T.; Pézolet, M. *Biomacromolecules* **2004**, *5*, 2247−2257.
(21) van Beek, J. D.; Hess, S.; Vollrath, F.; Meier, B. H. *Proc. Natl. Acad. Sci. U. S. A.* **2002**, *99*, 10266−10271.
(22) Kümmerlen, J.; van Beek, J. D.; Vollrath, F.; Meier, B. H. *Macromolecules* **1996**, *29*, 2920−2928.
(23) Holland, G. P.; Creager, M. S.; Jenkins, J. E.; Lewis, R. V.; Yarger, J. L. *J. Am. Chem. Soc.* **2008**, *130*, 9871−9877.
(24) Grubb, D. T.; Jelinski, L. W. *Macromolecules* **1997**, *30*, 2860−2867.
(25) Gosline, J.; Guerette, P.; Ortlepp, C.; Savage, K. *J. Exp. Biol.* **1999**, *202*, 3295−3303.
(26) Simmons, A. H.; Michal, C. A.; Jelinski, L. W. *Science* **1996**, *271*, 84−87.
(27) Ene, R.; Papadopoulos, P.; Kremer, F. *Vibr. Spectros.* **2011**, *57*, 207−212.
(28) Simmons, A.; Ray, E.; Jelinski, L. W. *Macromolecules* **1994**, *27*, 5235−5237.
(29) Vollrath, F.; Porter, D. *Appl. Phys. A: Mater. Sci. Process* **2006**, *82*, 205−212.
(30) Papadopoulos, P.; Ene, R.; Weidner, I.; Kremer, F. *Macromol. Rapid Commun.* **2009**, *30*, 851−857.
(31) Du, N.; Liu, X. Y.; Narayanan, J.; Li, L.; Lim, M. L. M.; Li, D. *Biophys. J.* **2006**, *91*, 4528−4535.
(32) Giesa, T.; Arslan, M.; Pugno, N. M.; Buehler, M. J. *Nano Lett.* **2011**, *11*, 5038−5046.
(33) Keten, S.; Zhiping, X.; Ihle, B.; Buehler, M. J. *Nat. Mater.* **2010**, *9*, 359−367.
(34) Tso, I.-M.; Wu, H.-C.; Hwang, I.-R. *J. Exp. Biol.* **2005**, *208*, 1053−1061.

(35) Tai, P.-L.; Hwang, G.-Y.; Tso, I.-M. *Int. J. Biol. Macromol.* **2004**, *34*, 237−243.
(36) Forman, R. A.; Piermarini, G. J.; Barnett, J. D.; Block, S. *Science* **1972**, *176*, 284−285.
(37) Otto, J. W.; Vassiliou, J. K.; Frommeyer, G. *Phys. Rev. B* **1998**, *57*, 3253−3263.
(38) Spain, I. L.; Dunstan, D. J. *J. Phys. E: Sci. Instrum.* **1989**, *22*, 923.
(39) Thirunavukkuarasu, K.; Hennrich, F.; Kamarás, K.; Kuntscher, C. A. *Phys. Rev. B* **2010**, *81*, 045424.
(40) Francis, E. A.; Durkó, G.; Jalsovszky, I.; Klupp, G.; Kamarás, K.; Kováts; Pekker, S.; Kuntscher, C. A. *Phys. Status Solidi B* **2012**, *249*, 2596−2599.
(41) Syassen, K. *High. Press. Res.* **2008**, *28*, 75−126.
(42) Dwivedi, A. M.; Krimm, S. *Macromolecules* **1982**, *15*, 186−193.
(43) Moore, W. H.; Krimm, S. *Biopolymers* **1976**, *15*, 2465−2483.
(44) Guinea, G. V.; Pérez-Rigueiro, J.; Plaza, G. R.; Elices, M. *Biomacromolecules* **2006**, *7*, 2173−2177.
(45) Mao, H. K.; Xu, J.; Bell, P. M. *J. Geophys. Res.* **1986**, *91*, 4673−4676.
(46) Yen, J.; Nicol, M. *J. Appl. Phys.* **1992**, *72*, 5535−5538.
(47) Stancik, A. L.; Brauns, E. B. *Vibr. Spectrosc.* **2008**, *47*, 66−69.
(48) Ene, R.; Papadopoulos, P.; Kremer, F. *Polymer* **2011**, *52*, 6056−6060.
(49) Ene, R.; Papadopoulos, P.; Kremer, F. *Polymer* **2010**, *51*, 4784−4789.